Theoretical and Applied Mechanics

University of Illinois at Urbana-Champaign

TAM

TAM Report No. 1016
UILU-ENG-2003-6004
ISSN 0073-5264

Burning rate of energetic materials with thermal expansion

by

Igor R. Kuznetsov
D. Scott Stewart

March 2003

Burning Rate of Energetic Materials with Thermal Expansion

Igor R. Kuznetsov, D. Scott Stewart*
Theoretical and Applied Mechanics, University of Illinois, Urbana, IL 61801, USA

March 4, 2003

Abstract

We present a study of one-dimensional flame structure of combusting solid propellants that focuses on the effects of variable material properties. A nonlinear heat equation is derived for a burning thermo-elastic solid with temperature-dependent specific heat, thermal expansion and thermal conductivity coefficients. It is then solved for different modelling approximations both analytically and numerically. Explicit expressions are derived for the regression rate of the propellant surface as functions of surface temperature. The full structure of propellant flame is studied to identify the influence of temperature dependent material properties on the regression rate, surface temperature and flame stand-off distance. Results are displayed for HMX and compared to experimental data and to numerical simulation with fair success.

Nomenclature:

k	thermal conductivity	μ, λ	elastic coefficients
ρ	density	T	temperature
m	mass flux	Z	reaction pre-exponential factor
α	thermal expansion coefficient	Q	heat release per unit mass
K	bulk modulus	Q_s	heat release less expansion losses
θ	thermal expansion scale		
Θ	reaction scale		*Subscripts:*
P	pressure	g	gas phase
n	preheat zone coordinate	o	base values at the room temperature
s	expansion zone coordinate	s	surface
ξ	reaction zone coordinate	f	flame (burnt gases)
C_v	specific heat		no subscript - condensed phase

*Corresponding author: D. Scott Stewart, Theoretical and Applied Mechanics, University of Illinois, 216 Talbot Laboratory, 104 S. Wright St., Urbana, IL 61081, USA (FAX: 217-244-5707, email: dss@uiuc.edu)

INTRODUCTION

A large number of models have been developed to describe steady combustion of homogeneous solid energetic materials. Over the past sixty years, the modelling approaches to the problem have focused on predicting solid propellant (SP) flame properties such as regression rate, flame stand-off distance and propellant surface temperatures as functions of externally imposed conditions and material properties of the propellant, its reactant and product gases. Some of the models that we mention below are classics, but little detailed modelling attention has been paid to such an important material property of the condensed phase as thermal expansion or to the effects introduced by temperature variation of thermal conductivity and specific heat. A complete model that incorporates all these important effects has not been established. It is important to construct new models that are analytically tractable to provide new insights into the influence of the additional effects on the overall combustion parameters such as regression rate, surface temperature and burnt gas temperature.

One of the first one-dimensional models of SP combustion was published in 1943 by Zel'dovich [1]. Earlier 'temperature discontinuity' theories explained SP surface decomposition by direct contact of 'hot' gas phase products with the 'cold' SP surface. In contrast, Zel'dovich introduced a continuous temperature profile and suggested that the temperature gradient and hence the heat flux experiences a jump across the solid-gas interface, commensurate with the heat of decomposition of the solid. Starting from the first principles and under an assumption of Arrhenius-type reaction in the limit of large activation energy in the gas phase, he derived analytical expressions for thermal profiles, reaction zone thickness and an expression for the regression rate of the burning energetic material. In terms of the mass flux, the latter is expressed as a function of gas parameters such as activation energy E_g, heat release Q_g, thermal conductivity k_g and density ρ_g, pre-exponential factor Z_g, and burnt gases temperature T_f:

$$m^2 = \frac{2\,k_g\,\rho_g\,Z_g\,R\,T_f^2\exp(-E_g/RT_f)}{E_g\,Q_g}\,. \tag{1}$$

This expression establishes the dependence between the regression rate (or the mass flux) and the parameters of the gas phase.

In 1959, Merzhanov and Dubovitski [2] examined the SP combustion from a viewpoint of processes that take place in the condensed phase. They considered an exothermic high activation energy reaction in the solid phase and resolved a narrow reaction zone near the

surface instead of reducing it to a discontinuity. As a result, a relationship between the regression rate and the surface temperature T_s, as well as condensed phase properties, was expressed (in terms of the mass flux) as follows

$$m^2 = \frac{k\,\rho\,Z\,R\,T_s^2\exp(-E/RT_s)}{E(C_v(T_s - T_0) - Q/2)}\,, \tag{2}$$

where C_v stands for the specific heat of the solid and T_0 is its temperature away from the combustion zone.

These two models have become the basis for most of the subsequent theoretical developments and have been modified and enhanced over the years by different authors to incorporate more complex physics. For example, Williams [3] presents a modified version of Merzhanov's model (2) to account for variable specific heat, more general reaction rate and varying concentration of the premixed fuel in the fresh region. Lengelle [4] takes into account detailed degradation reaction mechanism of polymers. He derives, using high activation energy asymptotics, a formula for the regression rate of combusting polymer with the correction for its partial degradation at the interface.

A more significant deviation from the classical model was suggested by Ward, Son and Brewster [5]. While studying the dependence of the HMX combustion regime on the gas phase activation energy, they used Merzhanov's formula to relate surface temperature to the mass flux. For the gas phase Arrhenius kinetics, they found that the low, and not high, activation energy approximation is more appropriate and derived, in that limit, a system of algebraic equations defining regression rate, surface temperature and gas phase reaction zone thickness.

A numerical study of the effect of variable thermal properties in the solid phase was presented by Blomshield and Osborn [6]. They showed that thermal penetration depth and regression rate can be changed if specific heat and thermal conduction depend on temperature. A number of authors considered detailed chemistry of the homogeneous propellant combustion and mechanics of the multi-phase melting layer that in some regimes separates solid and gaseous phases. An extensive list of references can be found in [7].

In [9], we suggested that thermal expansion stresses in the solid can produce work and in this way affect the thermal profile in the solid. It was shown that contribution from thermal expansion work can manifest itself in a narrow layer near the melting surface, where temperature gradients are high. Analytical expressions were derived for the thermal profiles in the bulk of the solid and temperature gradients at the surface. For typical solid propellant, interface temperature gradients can be increased by factor of 2 or more,

depending on the expansion parameters. Such changes in the temperature profile in the solid can then affect the burning rate of the propellant.

In this work we further study the influence of the temperature dependent material properties such as thermal expansion coefficient, specific heat and thermal conductivity on the burning rate and the entire flame structure. In what follows, we model the flame domain under the following assumptions. Solid phase is considered to be thermo-elastic, with one-step exothermic Arrhenius reaction. The gas phase is modelled by an ideal compressible inviscid reacting gas, also with one step Arrhenius kinetics. The study consists of two major parts.

In the first part of the paper, we establish the relationship between the surface temperature and the burning rate analogous to (2), with the correction for the variable material properties. Two formulations are presented (Fig.1), first for a material that has temperature dependent thermal expansion, but constant specific heat and thermal conductivity (MODEL A), and second, where all parameters are functions of temperature (MODEL B). For both models, the mass flux formula is derived asymptotically in the limit when chemical reaction is mostly confined to a zone of much smaller length than that of the thermal expansion zone. For a material that has reaction and thermal expansion zones of the same length, the relationship between regression rate and the surface temperature is obtained numerically.

In the second part, we use this relationship to provide appropriate boundary conditions for the equations in the gas phase, which we solve numerically for Lewis Number $Le = 1$. Numerical solution obtains the correct values of mass flux and surface temperature for given initial temperature, material properties and ambient pressure.

Finally, all the results are collected and discussed. Parametric study and comparison with the experimental data is carried out for a typical solid mono-propellant (HMX) to illustrate the significance of the thermal expansion and variable material properties.

BURNING RATE FOR MODEL A

Formulation

In [9], we present a model appropriate for a thermoelastic combusting solid. In a frame attached to the steadily regressing combustion front, a steady nonlinear heat equation in dimensional form is derived as

$$mC_v \frac{dT}{dn} = k \frac{d^2T}{dn^2} + \Phi_e + \Phi_r \ , \tag{3}$$

where Φ_e is the work term associated with thermal expansion and the term Φ_r accounts for chemical reaction in the solid. We choose the chemical reaction term to be of conventional Arrhenius form

$$\Phi_r = Q\rho Z \exp(-E/RT)\,.$$

Here Q is the heat release of the solid phase reaction, Z is a pre-exponential factor and ρ is local density in the solid. The thermal expansion term Φ_e was rigorously derived in [9], and in the one-dimensional case it reduces to

$$\Phi_e = T\frac{\partial\sigma}{\partial T}\frac{du}{dn} = -KT\left[\alpha + \frac{\partial\alpha}{\partial T}(T-T_0)\right]\frac{du}{dn}\,,$$

where σ is longitudinal stress, u is the speed of the material particle in a lab frame, K is the bulk coefficient and α is the thermal expansion coefficient. We choose a temperature sensitive functional form for $\alpha(T)$ that reflects a rapid change near the surface temperature

$$\alpha = \alpha_0\left[1 + b\exp(-\theta(1/T - 1/T_s))\right]\,, \tag{4}$$

where b reflects the magnitude of the change from the base value α_0, and θ measures the rate of change of $\alpha(T)$ near the surface temperature.

For convenience, we subsequently use a tilde to designate a dimensional quantity and the absence of tilde - a dimensionless one. Let $\tilde{n} = |\tilde{k}/(\tilde{m}\tilde{C_v})|\,n$, with the characteristic thermal conduction thickness for incompressible solid given by $|\tilde{k}/(\tilde{m}\tilde{C_v})|$. We take the surface temperature $\tilde{T_s}$ to be the characteristic temperature so that $\tilde{T} = \tilde{T_s}\,T$. (This choice sets the dimensionless surface temperature to be unity.) We introduce two additional non-dimensional parameters, a dimensionless activation energy for the reaction in the solid $\Theta = \tilde{E}/\tilde{R}\tilde{T_s}$ and a dimensionless parameter that characterizes the temperature sensitivity of the thermal expansion coefficient (analogous to activation energy) $\theta = \tilde{\theta}/\tilde{T_s}$. Then the dimensionless form of equation (3) becomes

$$-\frac{dT}{dn} = \frac{d^2T}{dn^2} + A\left[1 + b\,e^{-\theta(\frac{1}{T}-1)}\left(1 + \frac{\theta(T-T_0)}{T^2}\right)\right]^2 T\frac{dT}{dn} + \hat{\Lambda}\exp(-\Theta/T)\,. \tag{5}$$

Dimensionless parameters $\hat{\Lambda}$ and A are defined by

$$\hat{\Lambda} = \frac{\tilde{k}\tilde{Q}\tilde{\rho}\tilde{Z}}{(\tilde{m}\tilde{C_v})^2\tilde{T_s}}\,, \quad \text{and} \quad A = \frac{\tilde{\alpha}_0^2\tilde{K}^2\tilde{T_s}}{\tilde{C_v}(\tilde{\rho}_0(2\tilde{\mu}+\tilde{\lambda}) - \tilde{m}^2)}\,. \tag{6}$$

For a typical propellant combustion application, A can be approximated by

$$A = \frac{\tilde{\alpha}_0^2 \tilde{K}^2 \tilde{T}_s}{\tilde{C}_v \tilde{\rho}_0 (2\tilde{\mu} + \tilde{\lambda})}\,, \quad \text{since} \quad \frac{\tilde{m}^2}{\tilde{\rho}_0 (2\tilde{\mu} + \tilde{\lambda})} \ll 1\,. \tag{7}$$

One can readily estimate parameter A for such solid propellant as HMX. Using the values from Table 1, we find that its value is of the order of 10^{-3}. We will use this result shortly.

A closer look at the structure of equation (5) reveals the existence of two small length scales; one associated with thermal expansion and another with the reaction term. In general, two scenarios can be suggested. First, when the thermal expansion length scale is much larger then the reaction length scale and second, when they are of the same order of magnitude.

The first model is appropriate for the propellants with a very thin reaction zone, such as AP or HMX, and relatively wide thermal expansion zone, which corresponds to moderate values of $\tilde{\theta}$. It suggests that there exist three distinct layers (see Fig.1). The outer thermal conduction layer lies deep inside the solid, where temperature is well below the surface temperature. In that area, the chemical reaction source term in the equation is exponentially small, and the thermal expansion term is also small since the temperature dependence of the thermal expansion coefficient is exponentially weak, and A is sufficiently small. Hence, in the conduction layer one obtains a conventional exponential temperature profile. Closer to the hot surface, the thermal expansion comes into play. In this inner, or expansion layer, the thermal expansion term is balanced by the diffusion term. The closest to the surface of the burning propellant is the reaction layer. Here contribution from the chemical reaction term becomes large. However the thermal expansion term becomes relatively small again, and the balance in the reaction layer is maintained between reaction and diffusion terms. Assumptions of this model allow us to derive an asymptotic formula for the mass flux.

When the length scales of thermal expansion and reaction are comparable, there exist only two layers, the preheat layer, and the layer close to the interface, where thermal expansion and reaction terms are of the same order and balanced by the diffusion term. Within the limits of this model, one needs to rely on numerics to obtain the mass flux as a function of the surface temperature. We will return to the discussion of this model in the section were we describe the numerical solution of the coupled problem.

Asymptotic Solution for the Regression Rate

We look for an asymptotic solution of the equation (5) to derive a new version of Merzhanov's formula (2) that would account for the thermal expansion effect in the solid. The solid phase domain is subdivided into three zones. The reaction zone is closest to the interface and has

the characteristic length scale of the order $1/\Theta$. It is followed by a wider thermal expansion layer with non-dimensional length $1/\theta$.

To enforce this difference in scales, assume that

$$\theta/\Theta = o(1)\,. \tag{8}$$

If we assume an expansion for the preheat zone solution in the form

$$T_{preheat} = T^{(0)}(n) + \frac{1}{\theta}T^{(1)}(n) + \dots\,, \tag{9}$$

substitution into (5) obtains

$$\frac{dT^{(0)}}{dn} = -\frac{d^2T^{(0)}}{dn^2}, \qquad T^{(0)}(0) = 1, \qquad T^{(0)}(\infty) = T_0\,, \tag{10}$$

$$\frac{dT^{(1)}}{dn} = -\frac{d^2T^{(1)}}{dn^2}, \qquad T^{(1)}(\infty) = 0\,, \tag{11}$$

which generates the two-term preheat zone solution

$$T_{preheat}(n) = (1-T_0)e^{-n} + T_0 + \frac{1}{\theta}C_3e^{-n} + \dots\,. \tag{12}$$

We introduce the expansion layer coordinate $s = n\,\theta$ and look for a solution in the following form:

$$T_{expansion}(s) = 1 + \frac{1}{\theta}t^{(1)}(s) + \dots\,. \tag{13}$$

In this layer, diffusion always dominates over advection, which is uniformly small.

$$\frac{d^2t^{(1)}}{ds^2} + qe^{2t^{(1)}}\frac{dt^{(1)}}{ds} + \hat{\Lambda}\theta\exp^{-\Theta(1-\frac{1}{\theta}t^{(1)})} = 0\,, \quad q = Ab^2\theta(1-T_0)^2\,. \tag{14}$$

To balance the first two terms we consider a distinguished limit where $Ab^2\theta \sim O(1)$. Since A is physically estimated to be $O(10^{-3})$ and we anticipate an order of magnitude change in thermal expansion coefficient near the melt temperature (a factor of 5 to 10 is typical in plastics and salts, for example), we suppose that b is large, and we choose to study the formal asymptotic limit

$$A = \hat{A}\frac{1}{\theta^3}, \quad b = \hat{b}\theta, \quad \text{with} \quad \hat{A} = O(1),\, \hat{b} = O(1)\,, \quad \text{as} \quad \theta \to \infty\,. \tag{15}$$

The reaction term on the right hand side is an exponentially small term in the expansion layer. Indeed, the first correction in the asymptotic expansion of temperature should be

negative, since temperature away from the interface is less than $T_s = 1$. Therefore $t^{(1)} < 0$, and the reaction term is asymptotically small. The expansion layer equation reads

$$\frac{d^2 t^{(1)}}{ds^2} + q e^{2t^{(1)}} \frac{dt^{(1)}}{ds} = 0\,. \tag{16}$$

The solution of Eq. (16) is

$$t^{(1)}(s) = \frac{1}{2} \ln\left(\frac{-c_1}{\exp[2\,c_1(c_2 - s)] - q/2} \right), \qquad c_1 < 0\,. \tag{17}$$

Matching of the expansion and preheat solutions is straight forward and determines the constant c_1

$$c_1 = (T_0 - 1)\,. \tag{18}$$

The remaining constant c_2 will be obtained from matching with the reaction layer solution.

Next we match the thermal expansion layer solution to the solution in the reaction layer and ultimately determine the eigenvalue Λ. (In general, the eigenvalue appears in this problem because we have three boundary conditions for the second order differential equation on the reaction zone scale; two at zero and one at infinity. This requires a constraint that specifies the value of the mass flux.) In the reaction layer, equation (5) can be written as

$$-\frac{dT}{dn} = \frac{d^2 T}{dn^2} + \Phi_e + \Lambda \Theta^\beta e^{\Theta - \Theta/T}\,, \tag{19}$$

where Λ is defined by

$$\hat{\Lambda} = \Lambda \Theta^\beta \exp(\Theta)\,.$$

We introduce the reaction zone scale $\xi = n\Theta$ and look for a solution in the form

$$T_{reaction}(\xi) = 1 + \frac{1}{\Theta} \tau^{(1)}(\xi) + \dots\,, \tag{20}$$

On this scale both convection and thermal expansion terms are algebraically small, which leads to

$$\frac{d^2 \tau^{(1)}}{ds^2} + \Lambda \Theta^{\beta - 1} e^{\tau^{(1)}(\xi)} = 0\,. \tag{21}$$

To balance the terms consider a distinguished limit defined by $\beta = 1$. Finally, the reaction layer equation is

$$\frac{d^2\tau^{(1)}}{d\xi^2} + \Lambda \exp(\tau^{(1)}) = 0\,, \qquad \tau^{(1)}(0) = 0\,. \tag{22}$$

Formal matching of the reaction and expansion layer solutions gives the following:

$$T_{expansion}\Big|_2^{reaction} = 1 + \frac{1}{2\theta}\ln\frac{-c_1}{\exp(2c_1c_2) - q/2} - \frac{1}{\Theta}\frac{\exp(2c_1c_2)c_1}{\exp(2c_1c_2) - q/2}\xi\,,$$

$$T_{reaction}\Big|_2^{expansion} = \left(1 + \frac{1}{\Theta}\tau^{(1)}(\xi)\right)\Big|_2^{expansion}\,.$$

To match we require that

$$\ln\frac{-c_1}{\exp(2c_1c_2) - q/2} = 0 \quad \text{and} \quad \lim_{\xi\to\infty}\tau^{(1)}(\xi) = \frac{\exp(2c_1c_2)c_1}{\exp(2c_1c_2) - q/2}\xi\,,$$

which allows to determine that

$$c_2 = \frac{1}{2c_1}\ln(\frac{q}{2} - c_1) \quad \text{and} \quad \lim_{\xi\to\infty}\tau^{(1)}(\xi) = -(\frac{q}{2} + 1 - T_0)\xi\,, \tag{23}$$

So finally the expansion layer solution to two terms is written as

$$T_{expansion}(s) = 1 + \frac{1}{2\theta}\ln\left[\frac{1 - T_0}{(q/2 - T_0 + 1)e^{2(T_0-1)s} - q/2}\right] + \dots\,. \tag{24}$$

To find the eigenvalue Λ, multiply the reaction zone equation (22) by $d\tau^{(1)}/d\xi$ and integrate over the interval $(0;\infty)$:

$$\frac{1}{2}\left(\frac{d\tau^{(1)}}{d\xi}\right)^2\Big|_0^\infty = -\Lambda\int_0^\infty e^{\tau^{(1)}}\frac{d\tau^{(1)}}{d\xi}d\xi\,. \tag{25}$$

To evaluate the left hand side of this equality and to change the limits of integration on the right hand side we need to evaluate $d\tau^{(1)}/d\xi$ and $\tau^{(1)}$ at 0 and ∞.
The temperature perturbation $\tau^{(1)}$ must obey the boundary condition (22b) and matching condition (23). From the control volume energy balance on the condensed phase region we calculate the value of the temperature gradient at the gas-solid interface (at the edge of the reaction zone)

$$(1 - T_0) + T'(0) = Q_s\,, \qquad T'(0) = \frac{d\tau^{(1)}(\xi)}{ds}\Big|_{\xi\to 0} = (T_0 - 1) + Q_s\,,$$

where Q_s is the heat liberated (or consumed) in the chemical reaction, less the heat that was lost due to the thermal expansion of the solid

$$Q_s = \int_\infty^0(\Phi_r + \Phi_e)dn = Q - \int_{T_0}^1 A\left[1 + b\,e^{-\theta(\frac{1}{T}-1)}\left(1 + \frac{\theta(T - T_0)}{T^2}\right)\right]^2 T dT\,. \tag{26}$$

By matching the temperature derivative of the reaction layer solution to that of the expansion layer solution

$$T'_{reaction}(\xi) = \frac{1}{\Theta}\tau^{(1)'}(\xi) + \dots\,,$$

$$T'_{expansion}\Big|_2^{reaction} = -\frac{1}{\Theta}(1 - T_0 + \frac{1}{2}q)\,,$$

we obtain the condition

$$\lim_{\xi\to\infty}\tau^{(1)'}(\xi) = T_0 - 1 - \frac{1}{2}q\,.$$

Now we can integrate (22a) and obtain

$$-\frac{1}{2}\left[(1 - T_0 + \frac{1}{2}q)^2 - (T_0 - 1 + Q_s)^2\right] = \Lambda\int_0^{-\infty}\exp(\tau^{(1)})d\tau^{(1)} = -\Lambda\,,$$

$$\Lambda = (Q_s + q/2)(1 - T_0 - Q_s/2 + q/4)\,. \tag{27}$$

Recall that here

$$\Lambda = \frac{\tilde{k}\tilde{Q}\tilde{\rho}_s\tilde{Z}}{(\tilde{m}\tilde{C}_v)^2\tilde{T}_s}\Theta^{-1}\exp(-\Theta)\,, \quad \text{with} \quad T_0 = \frac{\tilde{T}_0}{\tilde{T}_s}\,, \quad \Theta = \frac{\tilde{E}}{\tilde{R}\tilde{T}_s}\,, \quad Q = \frac{\tilde{Q}}{\tilde{C}_v\tilde{T}_s}\,, \tag{28}$$

where the density at the surface of the solid is given by

$$\frac{\tilde{\rho}_0}{\tilde{\rho}_s} = 1 + \frac{\tilde{\alpha}\tilde{K}(\tilde{T} - \tilde{T}_0) - \tilde{P}_0}{2\tilde{\mu} + \tilde{\lambda}}\Big|_{T=T_s} = 1 + \frac{\tilde{\alpha}_0(b+1)\tilde{K}(\tilde{T}_s - \tilde{T}_0) - \tilde{P}_0}{2\tilde{\mu} + \tilde{\lambda}}\,. \tag{29}$$

Determining Λ from eqn. (27) is equivalent to finding the mass flux, which can be rewritten in dimensional form (dropping the tilde) as

$$m^2 = \frac{kQ\rho_s ZRT_s^2\exp(-E/RT_s)}{E\left[C_v(T_s - T_0) - Q_s/2 + \frac{q}{4}C_vT_s\right](Q_s + \frac{q}{2}C_vT_s)}\,. \tag{30}$$

This is a relationship between the mass flux and the surface temperature that is a modification of the Merzhanov's formula (2). It accounts for the effect of the thermal expansion, that is represented here by the term $q = Ab^2\theta(1 - T_0)^2$, as well as by the modified form of the heat release, Q_s, given by (26). If there is no thermal expansion, or in other words if the thermal expansion coefficient α is zero, then $q = 0$, $Q_s = Q$ and we arrive at the expression identical to (2).

BURNING RATE FOR MODEL B

Formulation

In this section the influence of temperature dependence of specific heat and thermal conductivity on the regression rate eigenvalue is studied. Motivation for such study comes from the experimental evidence [10], [11] that both thermal conductivity and specific heat can change as much as by 50 per cent over the range of the temperatures typical of solid propellants. Most mathematical models of solid propellant combustion neglect this temperature dependence and refer to them as relatively insignificant effects. Such simplification inevitably introduces modelling inaccuracy, so our goal here is to construct a simple model that does take these effects into account and to study how the results for the burning rates from such theories differ from those obtained for the constant material properties.

One of the obstacles one faces when trying to build a model for the material with variable material properties is that there is limited experimental data. Thermal expansion coefficient as a function of temperature is not well studied. The data on thermal conductivity and specific heat for the solid propellants are more readily available.

From the experimental data available [10], [11] we know that the thermal conductivity and specific heat of solid propellants are nonlinear functions of temperature. Propellants such as AP or HMX undergo phase changes in the preheat zone, before they decompose in the reaction zone. Those changes in crystalline structure introduce additional complexity to the temperature dependence of the material properties. Nevertheless, for the practical purposes, the linear functions of temperature are widely used to approximate the behavior of specific heat and thermal conductivity.

In [6], the linear dependence was used in a numerical study measuring the influence of variable thermal properties on propellant combustion. It was indicated that there exist significant differences between combustion parameters such as burn rate or temperature sensitivity calculated using the variable thermal properties and those calculated for constant parameters.

Here a similar linear approximation is used to derive an analog of (2) that accounts for the temperature dependence of thermal conductivity and specific heat. The form of such linear temperature dependence as suggested in [10] is

$$\tilde{C}_v(T) = \tilde{C}_v(1 + \tilde{a}(\tilde{T} - \tilde{T}_0)) = \tilde{C}_v(1 + a(T - T_0))\,, \tag{31}$$

$$\tilde{k}(T) = \tilde{k}(1 + \tilde{c}(\tilde{T} - \tilde{T}_0)) = \tilde{k}(1 + c(T - T_0))\,, \tag{32}$$

where $\tilde{k}$ and $\tilde{C}_v$ are the reference values at the ambient temperature. Then equation (3) takes the following form

$$-(1+a(T-T_0))\frac{dT}{dn} = (1+c(T-T_0))\frac{d^2T}{dn^2} + c\left(\frac{dT}{dn}\right)^2 + \Phi_e + \Phi_r\,, \tag{33}$$

where a and c are nondimensional linear fit parameters for specific heat and thermal conductivity, respectively.

As before, under the assumption of difference in the reaction and expansion scales, there exists an asymptotic solution for the regression rate, which is presented next.

Asymptotic Solution for the Regression Rate

To obtain the mass flux formula for the material with variable properties, we will closely follow the derivation in the previous section. In a similar manner, assumptions are made for the solution expansions in the three consecutive layers. In the preheat layer, to the first order

$$-(1+a(T^{(0)}-T_0))\frac{dT^{(0)}}{dn} = (1+c(T^{(0)}-T_0))\frac{d^2T^{(0)}}{dn^2} + c\left(\frac{dT^{(0)}}{dn}\right)^2\,. \tag{34}$$

By integrating this equation once and, using the fact that $lim_{n\to\infty} dT^{(0)}/dn = 0$, we get

$$\frac{dT^{(0)}}{dn} = \frac{(T_0-T^{(0)})(2-a(T_0-T^{(0)}))}{2(1+c(T^{(0)}-T_0))}\,, \tag{35}$$

Formal Van Dyke's two term matching of preheat and expansion zone solutions gives:

$$\left(\frac{dT^{(0)}}{dn} + \frac{1}{\theta}\frac{dT^{(1)}}{dn}\right)\Big|_2^s = \left(\frac{dt^{(1)}}{ds}\right)\Big|_2^n.$$

It can be shown that $dvT^{(1)}/dn$ does not generate a significant term that can influence the matching. To show that, consider

$$\frac{1}{\theta}\frac{dT^{(1)}}{dn}(\frac{s}{\theta}) = \frac{1}{\theta}\frac{dT^{(1)}}{dn}(0) + \frac{1}{\theta^2}\frac{d^2T^{(1)}}{dn^2}(0) + \dots$$

In this expression, $\frac{1}{\theta}\frac{dT^{(1)}}{dn}(0) = ord(1)$ when $\frac{1}{\theta}\frac{dT^{(1)}}{dn}(0) = ord(\theta)$. In other words, if

$$\lim_{n\to 0}\frac{dT^{(1)}}{dn}(n) = C\,, \tag{36}$$

where C is a finite number, then the statement is proven. To show that (36) holds, consider equation in the preheat zone at the next order:

$$\frac{d^2T^{(1)}}{dn^2}(1+c(T^{(0)}-T_0))+\frac{dT^{(1)}}{dn}(1+a(T^{(0)}-T_0)+2c\frac{dT^{(0)}}{dn})+T^{(1)}(c\frac{d^2T^{(0)}}{dn^2}+a\frac{dT^{(0)}}{dn})=0\,.$$

By expressing all derivatives of the zeroth order solution in terms of $T^{(0)}$, introducing a new independent variable $x = T^{(0)} - T_0$ and dropping the superscript of $T^{(1)}$, this equation can be rewritten as

$$x(2+ax)T_{xx}-2T_x\left(1+ax-\frac{cx(2+ax)}{1+cx}\right)+2T\left(-a+\frac{c}{1+cx}(1+ax-c\frac{x(2+ax)}{2(1+cx)})\right)=0\,.$$

Since $\lim_{n\to 0}\, x = 1 - T_0$, when n approaches zero, this equation is approximated by

$$a_1T_{xx}-a_2T_x+a_3T=0\,,$$

where a_i are some non-zero constants. Then the solution to this equation has the general form of

$$T=A_1\exp(\lambda_1 x)+A_2\exp(\lambda_2 x)\,,$$

which is bounded along with it's derivatives as x approaches the value of $(1 - T_0)$. Therefore,

$$\lim_{n\to 0}\frac{dT^{(1)}}{dn}=\lim_{n\to 0}\left(\frac{dT^{(1)}}{dx}\frac{dx}{dn}\right)=C\,;\qquad |C|<\infty\,.$$

where C is bounded.

Now we can match the derivatives of the expansion and preheat zones and hence specify the boundary condition for the expansion layer,

$$\lim_{n\to 0}\frac{dT^{(0)}}{dn}=\lim_{s\to\infty}\frac{dt^{(1)}}{ds}=\frac{(T_0-1)(2+a(1-T_0))}{2(1+c(1-T_0))}=\frac{(T_0-1)(1+C_{v_s})}{2k_s}\,.\qquad(37)$$

Here $k_s = (1 + c(1 - T_0))$, the nondimensional thermal conductivity at the surface, where $T = 1$. Similarly we define $C_{v_s} = (1 + a(1 - T_0))$, the nondimensional specific heat at the surface.

In the expansion layer, the balance of the terms with largest contribution gives

$$k_s\frac{d^2t^{(1)}}{ds^2}+qe^{2t^{(1)}}\frac{dt^{(1)}}{ds}=0\,,\qquad t^{(1)}(0)=0\,.\qquad(38)$$

The solution to this equation is

$$t^{(1)}(s) = \frac{1}{2}\ln\frac{-c_1}{(q/2k_s - c_1)e^{-2c_1 s} - q/2k_s}\,, \qquad \text{with} \qquad c_1 = \frac{(T_0-1)(1+C_{v_s})}{2k_s}\,, \tag{39}$$

where the constant c_1 was determined by enforcing the condition (37).

Taking the derivative of this solution we find the matching condition between the expansion and reaction zones

$$\lim_{s\to 0}\frac{dt^{(1)}}{ds} = \lim_{\xi\to\infty}\frac{d\tau^{(1)}}{d\xi} = \frac{(T_0-1)(1+C_{v_s}) - q}{2k_s}\,. \tag{40}$$

From the control volume balance over the entire solid domain we derive another boundary condition for the reaction layer:

$$\lim_{\xi\to 0}\frac{d\tau^{(1)}}{d\xi} = \frac{(T_0-1)(1+C_{v_s}) + 2Q_s}{2k_s}\,. \tag{41}$$

In the reaction layer, the equation is similar to (22):

$$k_s\frac{d^2\tau^{(1)}}{d\xi^2} + \Lambda\exp(\tau^{(1)}) = 0\,, \qquad \tau^{(1)}(0) = 0\,. \tag{42}$$

Integrating it and using (40) and (41), we determine the eigenvalue Λ:

$$\Lambda = \frac{1}{2k_s}(Q_s + q/2)\left[(1-T_0)(1+C_{v_s}) - Q_s + q/2\right]\,, \tag{43}$$

which is the same as to determine the mass flux. In the dimensional form and dropping the superscripts it can be expressed as

$$m^2 = \frac{2k(1+c(T_s-T_0))Q\rho_s ZRT_s^2\exp(-E/RT_s)}{E\left[C_v(2+a(T_s-T_0))(T_s-T_0) - Q_s/2 + \frac{q}{4}C_vT_s\right](Q_s + \frac{q}{2}C_vT_s)}\,. \tag{44}$$

where ρ_s is given by (29). The above should be viewed as an extension of mass flux formula (30) to the case of variable material properties. If a and c are set to zero, which corresponds to the constant specific heat and thermal conductivity, we retrieve (30).

COUPLED PROBLEM

Formulation

We have shown how the temperature-dependent thermal expansion and other material parameters can influence the relationship between the solid surface temperature and the

mass flux. The physics behind that dependence was so far based only on the processes that take place in the solid phase. For given initial temperature and chamber pressure we were able to derive the mass flux as a function of surface temperature. But for the whole flame structure, the fresh material temperature and chamber pressure, along with material properties, defines unique values of T_s and m that, of course, have to be related by the mass flux formula. To define those two unique parameters, one needs to solve the governing equations in the entire combustion domain, for both gas and solid phase. Therefore, the next step will be to supplement our theory with the gas phase solver, which will allow us to study what changes the thermal expansion will introduce to the overall parameters such as the burnt gas temperature and the mass flux as a function of pressure.

The primary focus of this work is to study the condensed phase phenomena, and not to capture the complexity of the detailed kinetics in the gas phase. We will, therefore, choose a simple classical gas phase model that will allow us to give a clear illustration of the theoretical developments above. The relationship between T_s and m that we have derived will be used to provide the appropriate boundary condition on the solid-gas interface and to numerically solve the gas phase equations. As a result, the mass flux eigenvalue and surface temperature should emerge as unique functions of the ambient pressure, initial temperature and material parameters.

Decomposition of the condensed phase was modelled in previous chapters as a unimolecular, irreversible reaction of the first order $A \rightarrow B$, where reactant A converts into intermediate species B, which then participate in the gas phase reaction. That reaction is modelled as a one step, bimolecular reaction $B + M \rightarrow C + M$, producing final products C. This reaction is first order in B and second order overall. The gas obeys ideal gas law, has constant specific heat and thermal conductivity and unity Lewis number. All the molecular weights are equal, and species diffusion is modelled by Fick's law. Specific heat of the gas is assumed to be equal to the base value of the specific heat of the solid phase. Gas phase occupies the left half-plain $(-\infty, 0)$.

With these assumptions, we write the gas phase species and energy conservation equations

$$\tilde{m}\tilde{C}_{p_g}\frac{d\tilde{T}}{d\tilde{x}} = \tilde{k_g}\frac{d^2\tilde{T}}{d\tilde{x}^2} + \tilde{Q}_g\rho_g^2\tilde{Z}_gY\tilde{T}^2\exp(-\tilde{\theta}_g/\tilde{T})\,, \tag{45}$$

$$\tilde{m}\frac{dY}{d\tilde{x}} = \tilde{\rho}_g\tilde{D}\frac{d^2Y}{d\tilde{x}^2} - \tilde{\rho_g}^2\tilde{Z}_gY\tilde{T}^2\exp(-\tilde{\theta}_g/\tilde{T})\,, \tag{46}$$

which we supplement with the equation

$$\tilde{\rho}_g = \tilde{p}\tilde{MW}/R\tilde{T}\,.$$

Here Y is the mass fraction of B in the gas phase, MW is the molecular weight of the gas. The boundary conditions (using the control volume balance for energy, Fig.6) are

$$\tilde{x} \to -\infty : \qquad \tilde{C}_{p_g}\tilde{T}_f = \tilde{C}_{p_s}\tilde{T}_0 + \tilde{Q}_s + \tilde{Q}_g, \qquad Y = 0\,; \tag{47}$$

$$\tilde{x} = 0 : \qquad \tilde{C}_{p_g}\tilde{T}_s = \tilde{C}_{p_s}\tilde{T}_0 + \tilde{Q}_s + \frac{\tilde{k}_g}{\tilde{m}}\frac{d\tilde{T}}{d\tilde{x}}|_{\tilde{x}=-0}\,, \qquad Y_s = 1 + \frac{\tilde{\rho}_g\tilde{D}}{\tilde{m}}\frac{dY}{d\tilde{x}}|_{\tilde{x}=-0}\,. \tag{48}$$

The assumption of $Le = 1$ reduces the system of two equations to one equation in temperature. In nondimensional form, it can be written [5] as

$$m\frac{dT}{dx} = \frac{d^2T}{dx^2} - D_g(T_f - T)exp(-\frac{E_g}{T_f - YQ_g}); \qquad T(0) = T_s, \quad T(-\infty) = T_f. \tag{49}$$

Numerical Solution of the Coupled Problem

Gas phase equations are solved iteratively as follows. The first guess for the surface temperature is made. Then we use the explicit formula (30) for MODEL A or (44) for MODEL B to make the first guess for the mass flux and the iteration procedure begins. We integrate the gas phase temperature equation from the equilibrium point at minus infinity toward the surface. As a result of this integration we can determine the temperature gradient at the interface. It is used to recalculate the value of T_s from the energy balance and then, from (30), the new value of m. Then integration of the gas phase is repeated. When iterations converge (the new T_s differs from the previous by value that is less then a preset tolerance), we obtain m and T_s, as well as the temperature gradient at the interface.

When the solid propellant exhibits thermal expansion on the same scale as chemical reaction, the premise for the asymptotic formulae (30), (44) becomes invalid. For both MODEL A and MODEL B, the value of the mass flux has to be calculated numerically for each value of the surface temperature, at each iteration step. This is done by another iteration loop that searches for the unique value of the mass flux that satisfies equation (3) with the following boundary conditions: $T(0) = T_s$, $T(\infty) = T_0$, $T'(0) = (T_0 - 1) + Q_s$ if the specific heat and thermal conductivity are constants. If they vary with temperature, we solve (33), with the temperature derivative at the interface calculated from (41).

RESULTS

Solid Phase

To illustrate the behavior of the solution, we use material properties of HMX (Table 1). Since the crystalline transformation in the bulk of material is not modelled, we use the properties of β-polymorph for the entire temperature range. The choice of the line-fit parameters a and b for MODEL B was based on the experimental data by Sewell at al. [15]. They provide data for the specific heat and thermal conductivity measured for temperatures up to about $500\,K$. When heated to higher temperatures, samples begin to decompose making data extraction procedure invalid. In our study we need to provide values of C_v, k at much higher pressures and temperatures than those in the experiment. For each given surface temperature T_s we choose the parameters a and c in such a way that the value of C_v and k change over the entire temperature domain (T_0, T_s) as much as they change over the range ($300\,K$, $500\,K$) in Sewell's experiment.

The thermal expansion coefficient that we use in this work is isotropic, and its temperature dependence is modelled by the exponential curve fit. This model applies to materials like HMX only as a first approximation. Laboratory experiments show that thermal expansion of the HMX grains is highly anisotropic, with linear expansion varying along the three axes of the crystal [14]. Here we will use an averaged linear expansion coefficient that is derived from the volumetric expansion data. Also, in the preheat zone, HMX suffers phase transition from one crystalline form to another, which causes a rapid contraction of the material. This effect has been averaged out by the exponential profile.

Next we discuss the choice of the thermal expansion characteristics θ, b and the effect that such choice can introduce to the model. Once again, b is the measure of change of the thermal expansion coefficient $\alpha(T_s)/\alpha_0$ over the entire range of temperature in the solid, and θ is the steepness of the $\alpha(T)$ profile, or a characteristic length of the thermal expansion layer. Due to the choice of the temperature scale T_s, the nondimensional values of $\Theta = E/RT_s$ and $\theta = \theta/T_s$ will vary as the surface temperature varies. Therefore, in the parametric studies we always refer to the reference value of θ at the temperature of $500\,K$.

Figure 2A compares the results for the mass flux based on Merzhanov's formula (2) to those obtained from (30) and (44) for $b = 5$, $\theta = 15$. We observe that due to the thermal expansion effect, the same value of regression rate is achieved at the higher surface temperature. For MODEL B, the profile lies even lower. The same results are compared with the numerical solution for the mass flux in Figure 2B and with the experimental

data in Figure 2D. The results from the asymptotic solution correspond rather well to the numerical solution, which means that chosen values of θ and b still satisfy the premise of the asymptotic model. As we increase the value of θ to $\theta = 50$, the deviation of the asymptotic result from numerics becomes significant (Figure 2C). For this value of θ, the expansion zone length becomes comparable to the reaction zone length: for HMX, the reference value of Θ is approximately equal to 50.

By further comparing numerical and asymptotic solutions we can define more clearly the range of parameters that are suitable for asymptotic solution. Figure 3 shows discrepancy (in per cent) between the regression rate obtained from asymptotics and from numerics. Figure 3A and 3B represent results for MODEL A. We see that zero error domain lies near $\theta = 20$ for the entire range of surface temperature and for b not larger than 10. Corresponding plots for MODEL B (Figure 3C and 3D) show more interesting behavior. While the range of $\theta = 15$ to $\theta = 20$ still gives relatively small error for most of the surface temperature domain, Figure 3D reveals that θ in that range is only 'good' for values of b between 5 and 7. The model is more restrictive on values of b, which we agreed (15) to be of the same order of magnitude as θ.

What are the other criteria that we can use to specify values of θ and b? Available data on materials like PMMA, for example, shows [16] that it exhibits a nearly 7-fold increase in the thermal expansion coefficient over a temperature range of 250 degrees Kelvin and a significant rise of its temperature derivative near the melting point. If we were to fit the $\alpha(T)$ curve for PMMA with an exponential similar to (4), the values of θ, b would be those close to 10.

Another piece of information comes with data on the HMX melt density for different melting temperatures. According to Sewell [15], density varies from 1650 kg/m^3 at 550 K to 1488 kg/m^3 at 800 K, which corresponds to 13 to 21 per cent change from the chosen base HMX density of 1900 kg/m^3. In our model such density change (accounted for by the thermal expansion) should not be larger than that reported by Sewell. Figure 4 shows such change (in per cent) calculated from (29) by the asymptotic model, as a function of T_s and b. As we see, for the range of parameters we are interested in (near $b = 5$) the density change is not more than 5 per cent. Additional expansion can be due to the crystalline phase transitions in the preheated material.

As we study the sensitivity of the model to the variation of thermal expansion parameters, we find an interesting threshold of values of θ and b. Figure 5 shows the total heat release in the solid phase of HMX Q_s, calculated from (26), as a function of these parame-

ters. What is shown there, is an absolute value of heat consumed by the thermal expansion ($Qs - Q$) as the percentage of the heat generated by the deflagration Q. Interestingly, as parameters increase, the net effect can become negative, or, in other words, the total effect of all the processes in the solid phase will become endothermic (for example, at θ=20, b=8). The transformation of HMX to gases is considered to be exothermic [8], based on the experimental evidence [13] that the chemical reaction heat release is much greater than the phase transformation heat losses. With the thermal expansion effect coming into picture, that subtle balance can be changed and the transformation of HMX in the condensed phase can become overall endothermic.

Coupled Problem

Overall temperature profiles for $P = 50\,Atm$ are presented in Figure 7. As we look at the difference between the numerical results obtained for MODEL A and for the material with no thermal expansion (base case) (7A), we observe that the MODEL A yields temperature of the burnt gases that has decreased from the base value of $2730\,K$ by approximately $180\,K$. That decrease is the measure of the energy that was consumed by expansion work in the solid. Figure 7B shows the same profile near the interface, where the surface temperature has to be higher for MODEL A then for the base material to sustain the same regression rate of $10\,mm/s$. As we have expected, thermal expansion increased the absolute value of the temperature gradient beneath the surface of the propellant. Deep inside the bulk of the propellant, the change in the temperature profiles is not very significant.

On the contrary, 7C shows that for MODEL B the temperature profile in the solid lies much lower than that of the base material. Variable C_v, k combined with thermal expansion lead to further steepening of the temperature profile beneath the surface and decrease the penetration depth of the temperature profile. Surface temperature becomes even higher than that for MODEL A, which is not surprising after we observed the results in Figure 2. The burnt temperature of the gases in the gas phase for MODEL B remains the same as that for MODEL A, as the expansion heat loss term in (26) is not affected by variability of the specific heat and thermal conductivity. Gas phase profiles for both MODEL A and MODEL B reveal smaller flame stand-off distance than that for the base (no expansion, constant parameters) material.

Before displaying more results of the coupled problem solution, we need to address the issue of the choice of gas phase activation energy θ_g. While it is generally accepted that activation energy of the solid phase chemical reaction of the SP is high, there are two

different opinions concerning that of the gas phase reaction. The most common approach to the simplified gas phase kinetics modelling for combusting energetic solids is what is called the high activation energy asymptotics, or AEA. Nevertheless, solutions obtained by such standard method are not always in a good accord with the experimental data. This fact prompted Ward at al. [5] to suggest that in the reaction the low activation energy limit is more appropriate. In that limit, the thermal profiles in the gas, as well as the burning rate data obtained by analysis, give a somewhat better agreement with experiment.

We test our model in two limits, for high and low activation energy. In both cases, we calibrate a model by adjusting the gas phase frequency factor in such a way that for initial temperature $T_o = 293\ K$ and pressure of $P = 50\ Atm$, the burning rate is equal to 10 mm/s [8]. That parameter is then held constant and the model is tested at other values of pressure. A finer tuning may be justified to calibrate the model for each pair of (b, θ), but was not attempted here.

Flame stand-off distance is presented in Figure 8. For all cases, the distance was taken at $T = 0.999\,T_f$, and $\theta = 15$, $b = 5$. Low activation energy calculation gives a better result than the high activation energy limit for both base material and for MODEL A. We observe that thermal expansion effect leads to considerable decrease of the gas flame thickness for the same values of pressure.

Figure 9 shows burning rate as a function of pressure, for $\theta = 15$, $b = 5$ for MODEL A. We see that the low activation energy limit matches experimental data more closely.

CONCLUSIONS

Two qualitative models (with constant and variable C_v, k) of the solid propellant with thermal expansion were suggested. In a limit of separable thermal expansion and chemical reaction length scales, explicit expressions for the mass flux as a function of the burning propellant surface temperature were derived for both models using the method of matched asymptotics. For materials with comparable characteristic length scales, numerical model was used to obtain the mass flux in terms of surface temperature.

With HMX as a representative energetic material, it was observed that the thermal expansion results in a regression rate decrease for the entire range of surface temperatures. It was shown that the thermal expansion work leads to heat losses, as well as the swelling of the material, in a thin layer near the propellant surface. Due to these losses, the overall energy balance in the solid phase can become endothermic, provided the expansion is relatively

strong. Also, the burnt gas temperature is influenced by the heat losses and becomes smaller with stronger expansion.

These results were used to provide proper boundary condition on the solid-gas interface and solve the coupled problem. The coupled gas-solid model was tested in two limits of the gas phase activation energy. The low activation energy limit shows better correspondence with experimental data for the regression rate as a function of pressure. Flame stand-off distance as a function of pressure was calculated and it was observed that the stand-off distance becomes smaller due to the thermal expansion for both activation energy limits.

Application of current model to real solid propellants has to be consistent with its purpose, which is to make a qualitative description of the thermal expansion influence on the combustion regime. When calculating values of the regression rate of HMX and using its material properties we need to understand the amount of uncertainty we deal with while modelling thermal expansion. The effect itself, though important for the combustion process, has not been studied in great detail. Only base values of the thermal expansion coefficient can be found in the literature. Hence the assumption of the form for the thermal expansion coefficient [9].

These qualitative results of the model provide a better understanding of the thermal expansion and the effect it can have on the overall combustion process, and can be used in the future studies of energetic materials deflagration.

Table 1. Parameter Values Used for HMX

$\tilde{k}$	=	$0.2(W/mK), [7]$	$\tilde{k}_g$	=	$7.0 \times 10^{-2}(W/mK), [7]$
$\tilde{C}_p$	=	$1.4 \times 10^3(J/kgK), [7]$	$\tilde{C}_{p_g}$	=	$1.4 \times 10^3(J/kgK), [7]$
$\tilde{\rho}_0$	=	$1900(kg/m^3), [7]$	$\tilde{Q}_g$	=	$3 \times 10^6(J/kg), [7]$
$\tilde{Q}$	=	$4.0 \times 10^5(J/kg), [7]$	$\tilde{MW}$	=	$34.2(kg/mole), [5]$
$\tilde{\alpha}_0$	=	$4.0 \times 10^{-5}(1/K), [7]$	$\tilde{\lambda}$	=	$8.6 \times 10^9(Pa), [15]$
$\tilde{K}$	=	$12.4 \times 10^9(Pa), [15]$	$\tilde{\mu}$	=	$7.8 \times 10^9(Pa), [15]$
$\tilde{Z}$	=	$14.5 \times 10^{16}(1/s), [7]$			
$\tilde{E}$	=	$2.1 \times 10^5(J/mole), [7]$			

ACKNOWLEDGEMENTS

The University of Illinois Center for Simulation of Advanced Rockets research program is supported by the US Department of Energy through the University of California under sub contract B341494. D. S. Stewart has also been supported by Los Alamos National Laboratory, DOE/LANL I2933-0019.

References

[1] Zel'dovich, Ya. B., *On the Theory of Combustion of Powders and Explosives*, Zurnal Experimental'noi i Teoreticheskoi Fisiki, vol 12, No.11-12, 1942, pp. 498-524.

[2] Merzhanov, A. G. and F. I. Dubovitskii, *The Theory of Stationary Combustion in Powders*, Proc. USSR Acad. Sci., Vol.129, 1959, pp. 153-156.

[3] Williams, F. A. *Combustion Theory*, 2nd Ed., Addison-Wesley, New York, 1985, pp. 238-243.

[4] Lengelle, G. *Thermal Degradation Kinetics and Surface Pyrolysis of Vinyl Polymers*, AIAA J., 8:1989-1998 (1970)

[5] Ward, M.J., Son, S.F. and M.Q. Brewster, *Steady Deflagration of HMX with Simple Kinetic*. Combustion and Flame J., Vol. 114, 1998.

[6] Blomshield, F.S. and J.R. Osborn, *Effect of Variable solid Phase Properties on Propellant Combustion*, Acta Astronautica, Vol.12, No.12, pp. 1017-1025 (1985).

[7] *Solid Propellant Chemistry, Combustion and Motor Interior Ballistics*, in Progress in Astronautics and Aeronautics, Vol. 185, AIAA Inc., 2000.

[8] Lengelle, G., Duterque, J. and F. Trubert, *Physico-Chemical Mechanisms of Solid Propellant Combustion*, Progress in Astronautics and Aeronautics, Vol. 185, AIAA Inc., pp. 287-334 (2000).

[9] Kuznetsov, I.R. and D.S. Stewart, *Modeling the Thermal Expansion Boundary Layer During the Combustion of Energetic Materials.* Combustion and Flame J., 126:1747-1763 (2001).

[10] Zanotti, C. and A. Volpi, *Measuring Thermodynamic Properties of Burning Propellant*, in Progress in Astronautics and Aeronautics, Vol. 143, 1992, pp. 145-198.

[11] Hanson-Parr, D.M. and T. P. Parr, *Thermal Properties Measurements of Solid Rocket Propellant Oxidizers and Binder Materials as a Function of Temperature.* Journal of Energetic Materials, Vol.17, 1999, pp. 001-047.

[12] Parr T. P. and D.M. Hanson-Parr, in *Decomposition, Combustion and Detonation Chemistry of Energetic Materials,* (T. B. Brill, T. P. Russel, W. C. Tao, and R. B. Wardle, Eds.), MRS, Pittsburg, 1996, pp. 207-219.

[13] Trubert, J. F., *Analysis of the Condensed Phase Degradation Gases of Energetic Binders*, La Recherche Aerospatiale, No. 2, 1989, pp.69-79; also AGARD CP 391, Sept. 1985.

[14] Herrman, M., Engel, W. and N. Eisenreich, *Thermal Expansion, Transitions, Sensitivities and Burning Rates fo HMX*, Propellants, Explosives, Pyrotechniques, Vol.17, 1992, pp. 190-192.

[15] Sewell, T.D., Bedrov, D. and G. D. Smith, *Atomic Predictions of Thermophysical and Mechanical Properties of Liquid and Cristalline HMX*, GRC on Energetic Materials, 2000.

[16] *Thermodynamical Properties of Matter.* TPAC Data Series, Vol. 13, Plenum Publishing, New York, NY, 1997 pp. 1470-1473.

[17] Boggs, T.L., *The Thermal Behavior of RDX and HMX*, in Fundamentals of Solid Propellant Combustion, edited by K.K. Kuo and M. Summerfield, Vol. 90, Progress in Astronautics and Aeronautics, AIAA, New York, pp. 121-175 (1984).

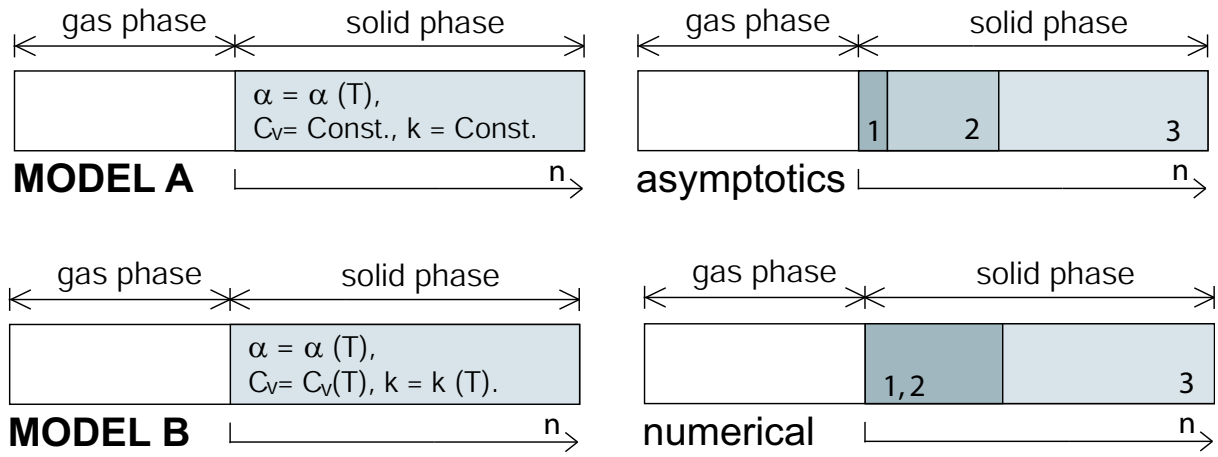

Figure 1: In MODEL A, solid propellant is modelled as elastic solid with thermal expansion and constant specific heat C_v, thermal conductivity k. In MODEL B, C_v and k are linear functions of temperature. Depending on the thermal expansion parameters, regression rate for each of the two models can be calculated either numerically, or using matched asymptotics. For the asymptotic solution, solid is subdivided into three zones: reaction zone(1) is followed by expansion zone(2) and preheat zone(3). When reaction and thermal expansion take place on the same length scale, numerical solution is used.

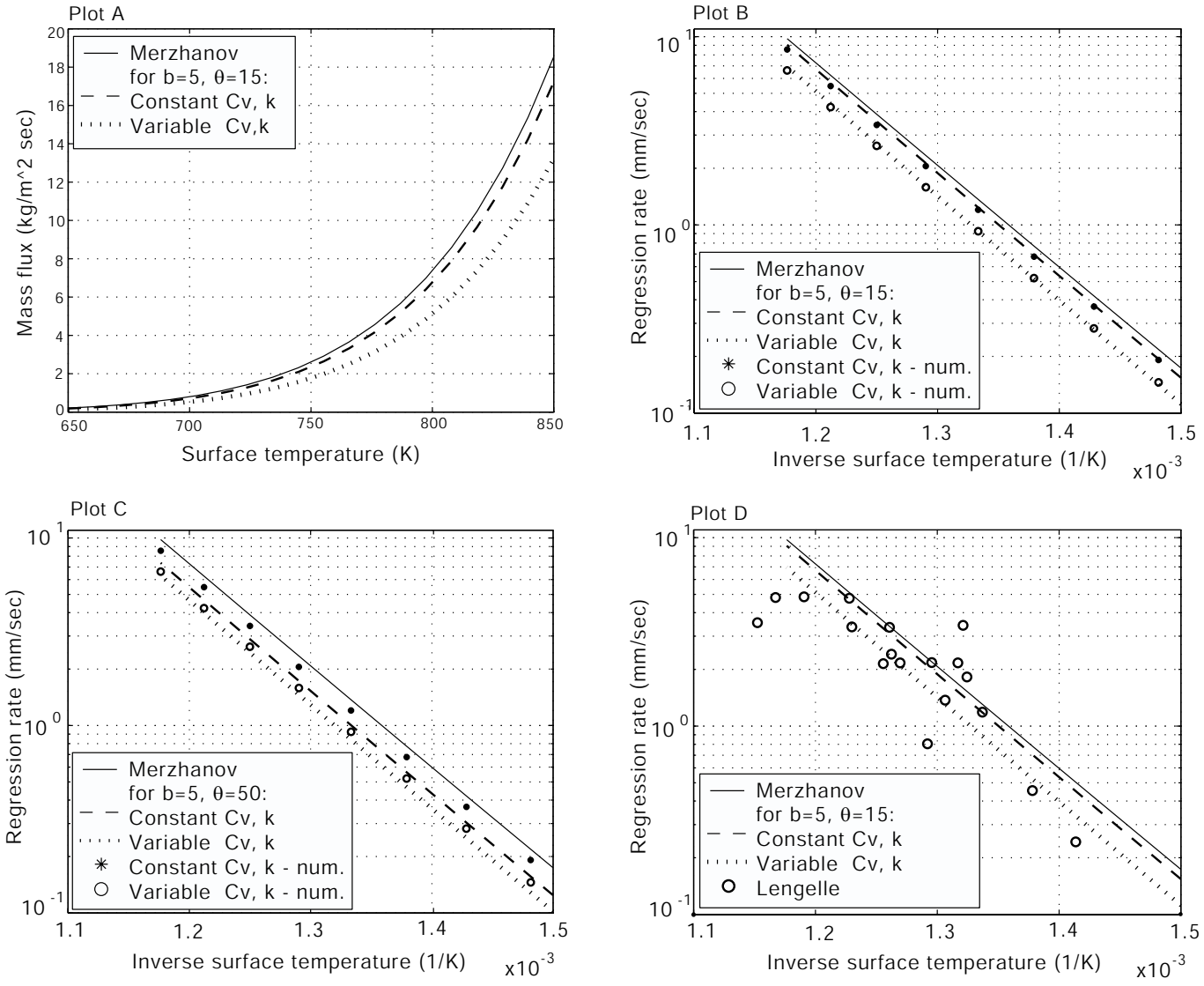

Figure 2: a) Mass flux as a function of surface temperature for Merzhanov's formula (solid line), MODEL A(dashed line) and MODEL B(dotted line); b), c) Comparison of the regression rate obtained from asymptotic formula to the numerical solution; d) Comparison to the experimental data. For all plots, $P = 50\,Atm$

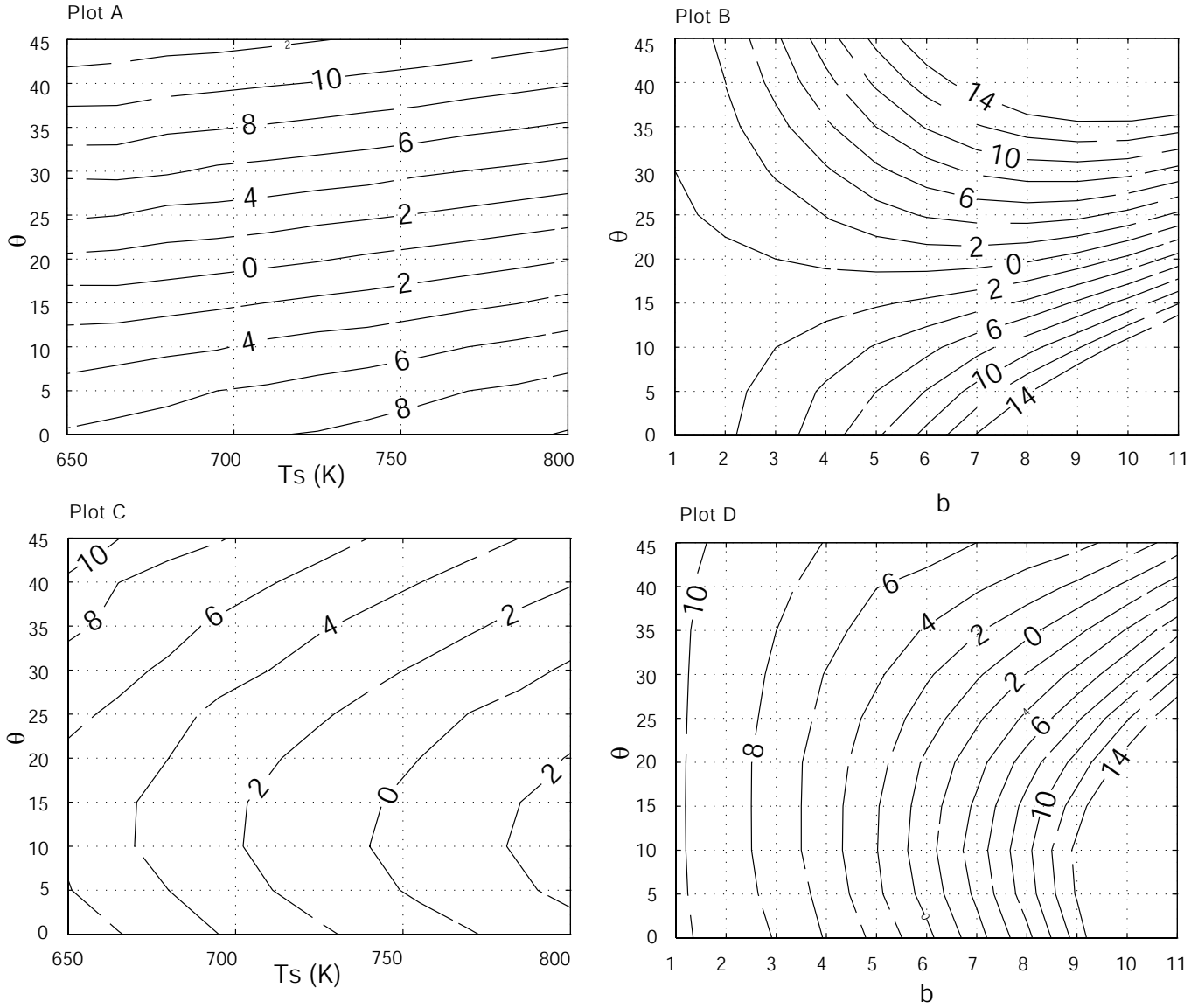

Figure 3: Deviation (in per cent) of the regression rate by asymptotic formula from numerically obtained regression rate as function of b, θ and T_s. a), b) MODEL A; c), d) MODEL B.

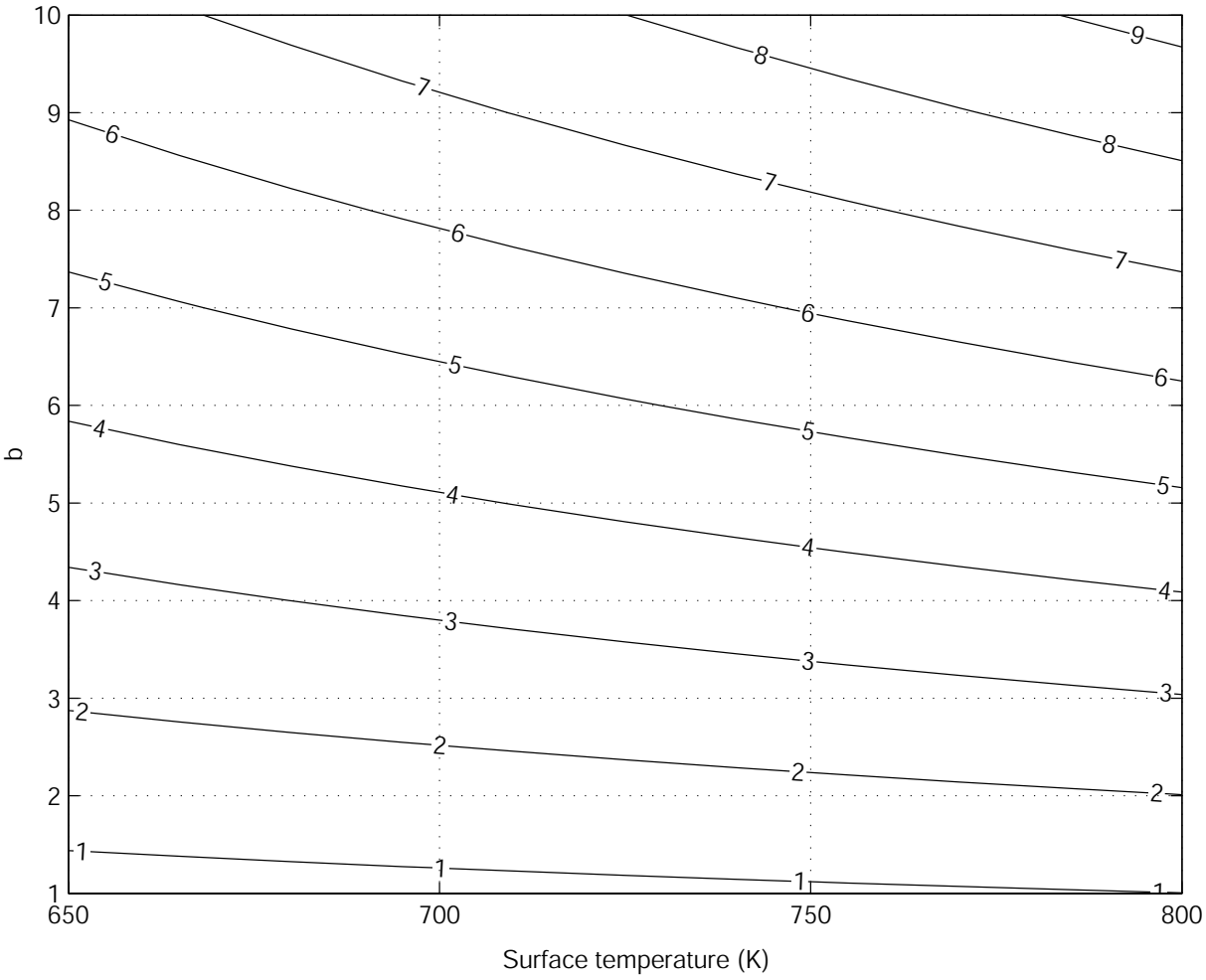

Figure 4: Density change (in per cent) from the reference density ρ_0, as function of b and T_s, at $P = 50\,Atm$.

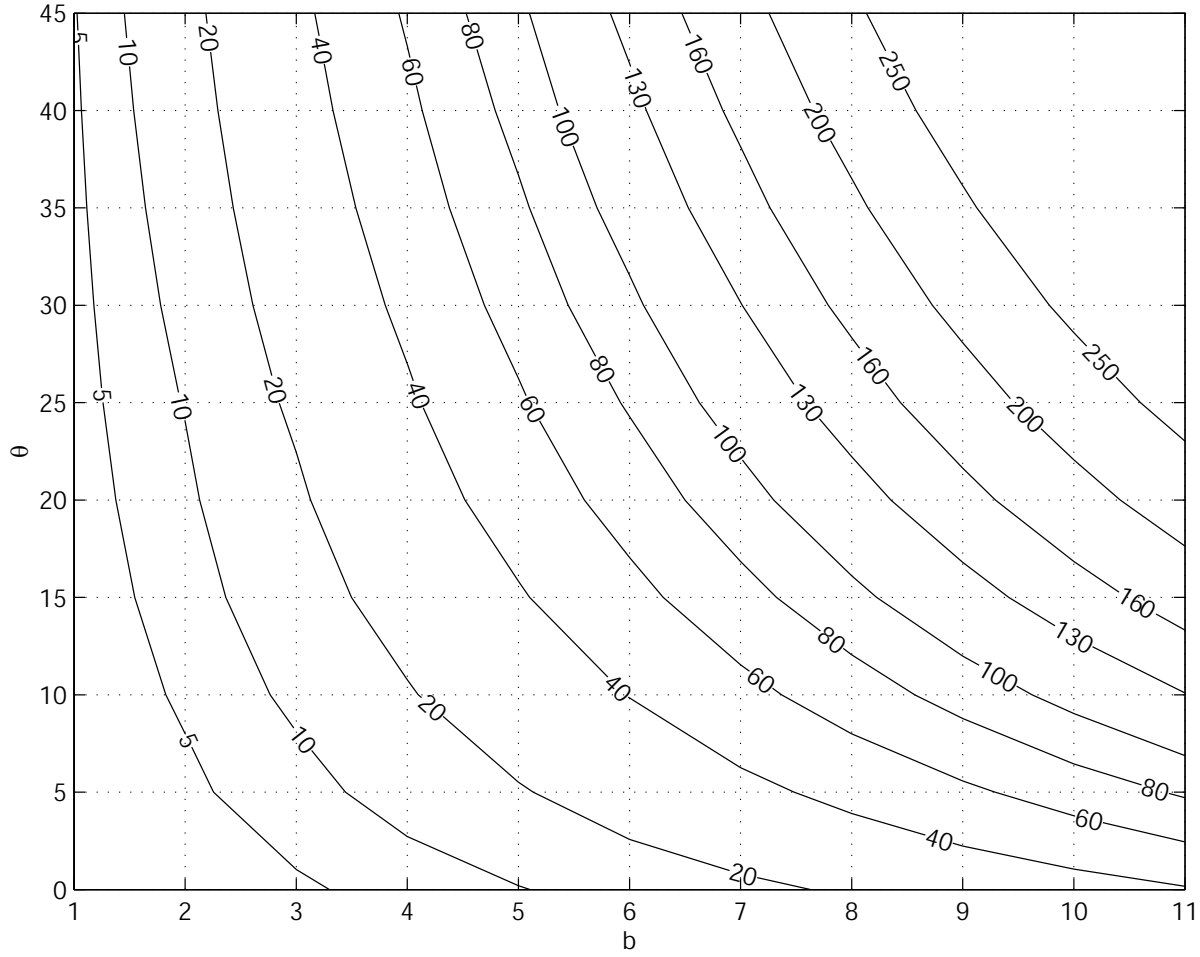

Figure 5: Heat loss due to thermal expansion (in per cent of the heat release due to chemical reaction), as a function of thermal expansion parameters b, θ, at $P = 50$ Atm.

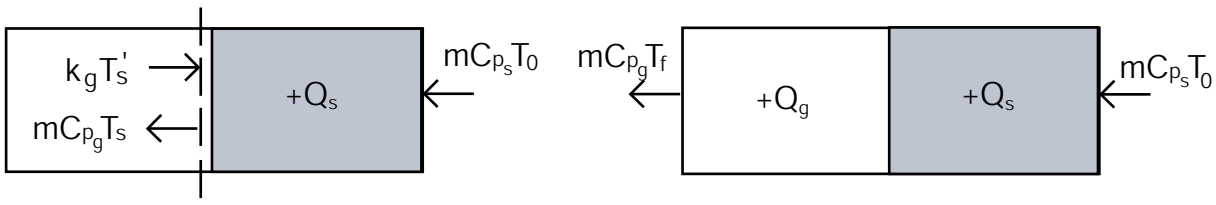

Figure 6: Control volume energy balance for the gas phase boundary conditions at the surface and at minus infinity.

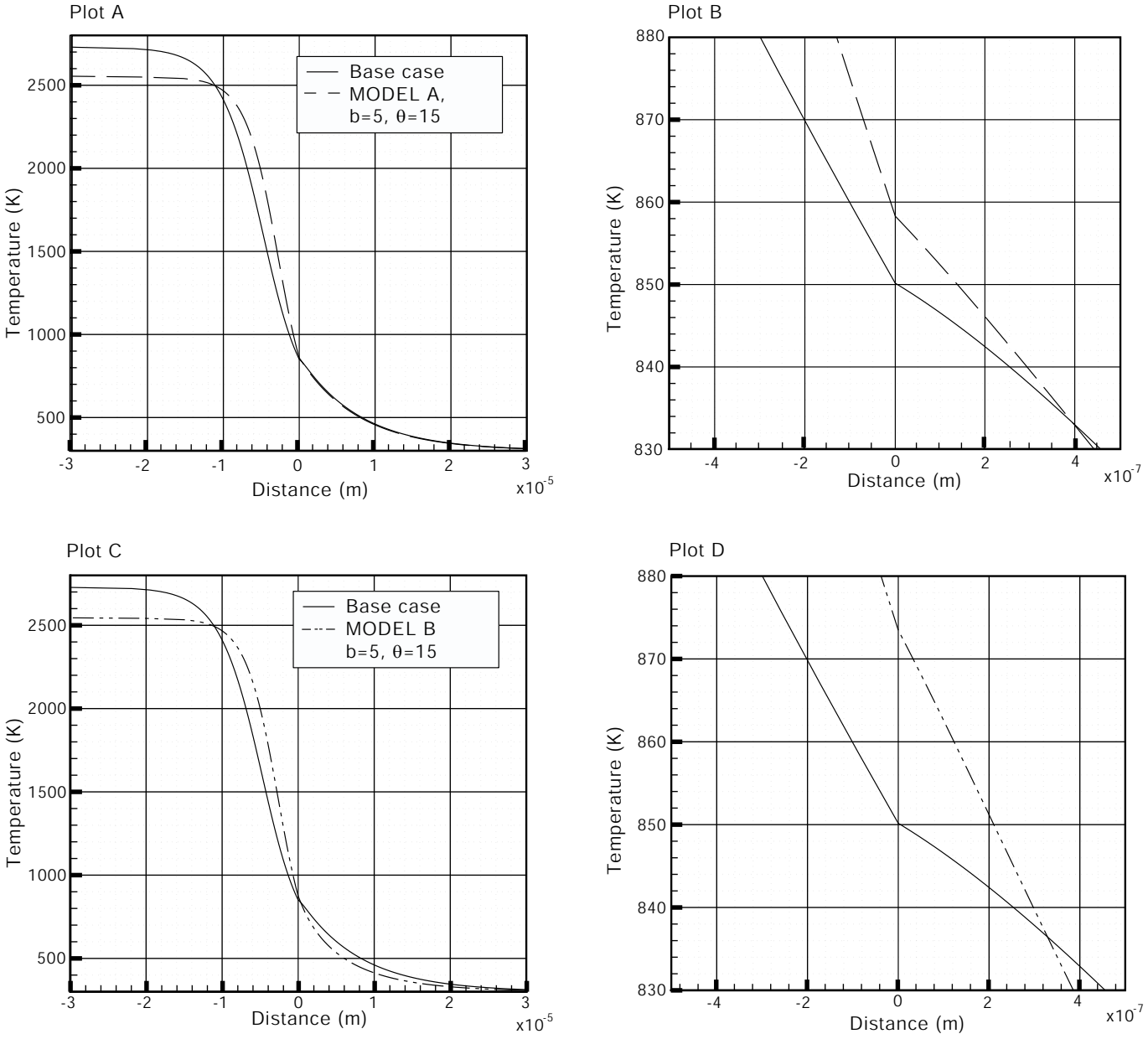

Figure 7: Temperature profiles for material with no thermal expansion and constant material properties (solid line: Base case) compared to temperature profile by MODEL A (a,b), and to temperature profile by MODEL B (c, d) .

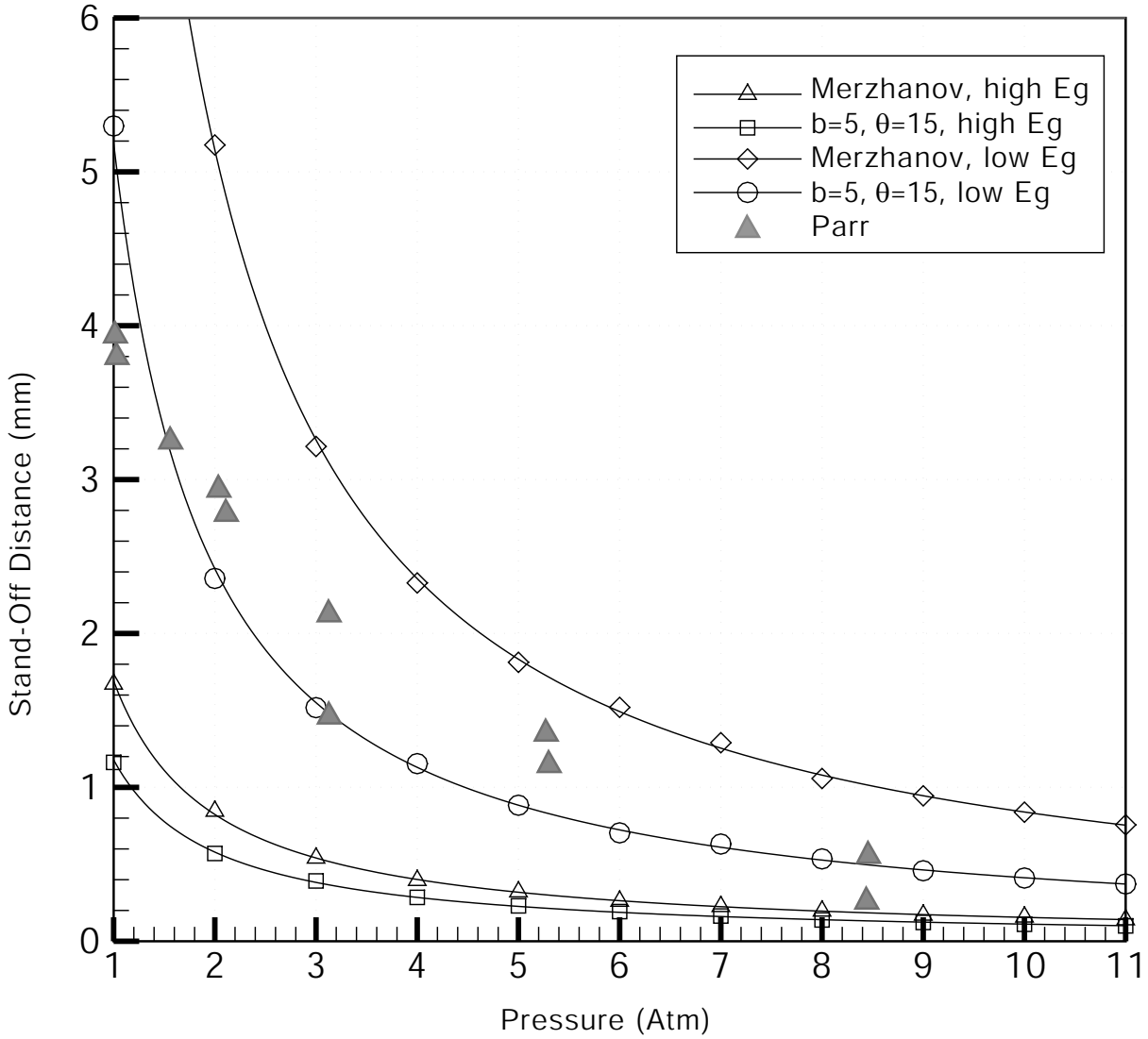

Figure 8: Gas flame stand-off distance ($T = 0.999\,T_f$); Comparison of calculations using Merzhanov's formula and MODEL A ($\theta = 15$, $b = 5$), for both high ($E_g = 40{,}000$) and low (E_g =10) gas phase activation energy limits. Experimental data by Parr and Hanson-Parr [12] .

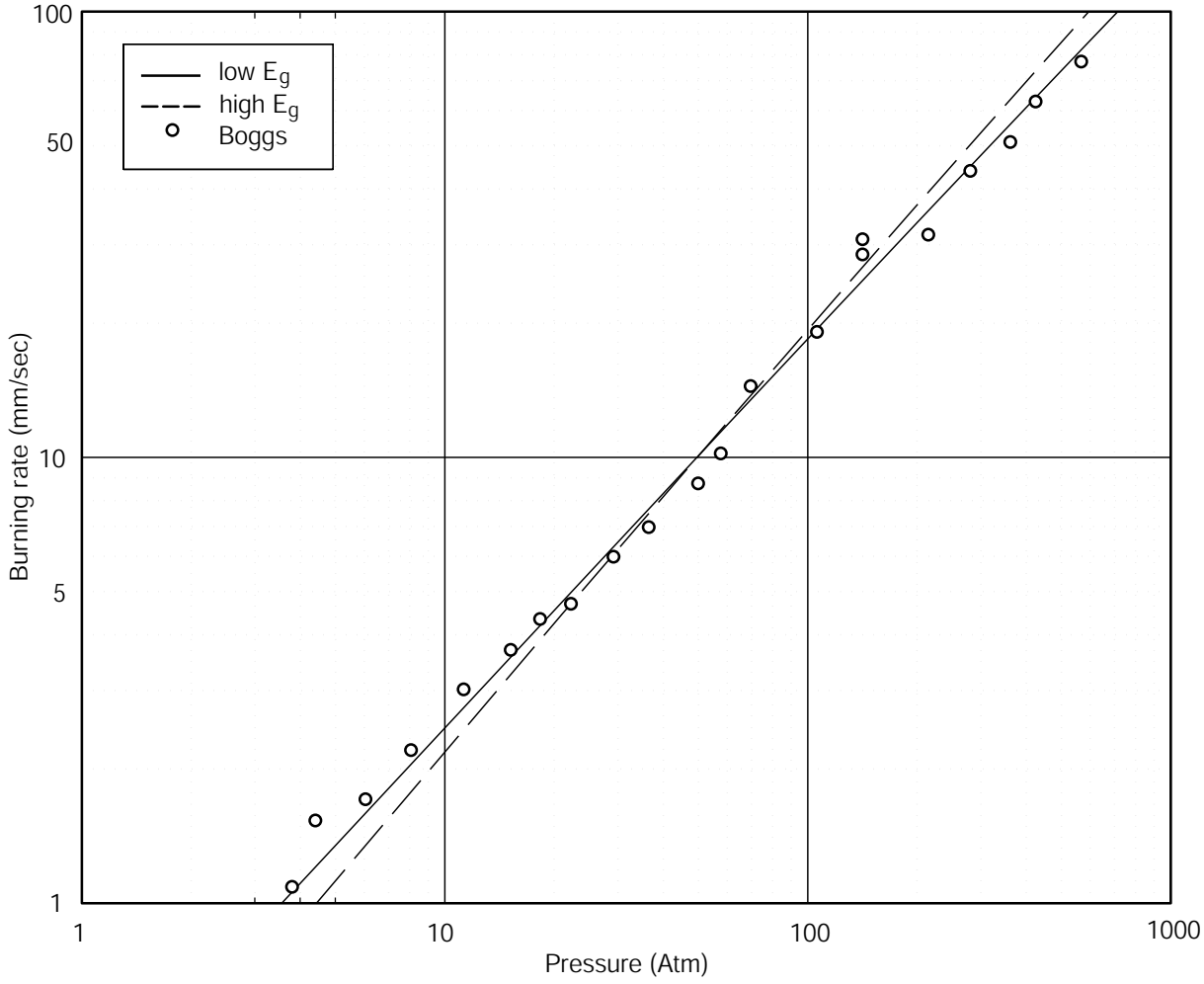

Figure 9: MODEL A: Burning rate of HMX as a function of pressure, for high ($E_g = 40{,}000$) and low (E_g =10) activation energy. $\theta = 15$, $b = 5$. Experimental data by Boggs [17].

List of Recent TAM Reports

No.	Authors	Title	Date
933	Sakakibara, J., Hishida, K., and W. R. C. Phillips	On the vortical structure in a plane impinging jet—*Journal of Fluid Mechanics* **434**, 273–300 (2001)	Apr. 2000
934	Phillips, W. R. C.	Eulerian space–time correlations in turbulent shear flows—*Physics of Fluids* **12**, 2056–2064 (2000)	Apr. 2000
935	Hsui, A. T., and D. N. Riahi	Onset of thermal–chemical convection with crystallization within a binary fluid and its geological implications—*Geochemistry, Geophysics, Geosystems* **2**, 2000GC000075 (2001)	Apr. 2000
936	Cermelli, P., E. Fried, and S. Sellers	Configurational stress, yield, and flow in rate-independent plasticity—*Proceedings of the Royal Society of London A* **457**, 1447–1467 (2001)	Apr. 2000
937	Adrian, R. J., C. Meneveau, R. D. Moser, and J. J. Riley	Final report on 'Turbulence Measurements for Large-Eddy Simulation' workshop	Apr. 2000
938	Bagchi, P., and S. Balachandar	Linearly varying ambient flow past a sphere at finite Reynolds number—Part 1: Wake structure and forces in steady straining flow	Apr. 2000
939	Gioia, G., A. DeSimone, M. Ortiz, and A. M. Cuitiño	Folding energetics in thin-film diaphragms—*Proceedings of the Royal Society of London A* **458**, 1223–1229 (2002)	Apr. 2000
940	Chaïeb, S., and G. H. McKinley	Mixing immiscible fluids: Drainage induced cusp formation	May 2000
941	Thoroddsen, S. T., and A. Q. Shen	Granular jets—*Physics of Fluids* **13**, 4–6 (2001)	May 2000
942	Riahi, D. N.	Non-axisymmetric chimney convection in a mushy layer under a high-gravity environment—In *Centrifugal Materials Processing* (L. L. Regel and W. R. Wilcox, eds.), 295–302 (2001)	May 2000
943	Christensen, K. T., S. M. Soloff, and R. J. Adrian	PIV Sleuth: Integrated particle image velocimetry interrogation/validation software	May 2000
944	Wang, J., N. R. Sottos, and R. L. Weaver	Laser induced thin film spallation—*Experimental Mechanics* (submitted)	May 2000
945	Riahi, D. N.	Magnetohydrodynamic effects in high gravity convection during alloy solidification—In *Centrifugal Materials Processing* (L. L. Regel and W. R. Wilcox, eds.), 317–324 (2001)	June 2000
946	Gioia, G., Y. Wang, and A. M. Cuitiño	The energetics of heterogeneous deformation in open-cell solid foams—*Proceedings of the Royal Society of London A* **457**, 1079–1096 (2001)	June 2000
947	Kessler, M. R., and S. R. White	Self-activated healing of delamination damage in woven composites—*Composites A: Applied Science and Manufacturing* **32**, 683–699 (2001)	June 2000
948	Phillips, W. R. C.	On the pseudomomentum and generalized Stokes drift in a spectrum of rotational waves—*Journal of Fluid Mechanics* **430**, 209–229 (2001)	July 2000
949	Hsui, A. T., and D. N. Riahi	Does the Earth's nonuniform gravitational field affect its mantle convection?—*Physics of the Earth and Planetary Interiors* (submitted)	July 2000
950	Phillips, J. W.	Abstract Book, 20th International Congress of Theoretical and Applied Mechanics (27 August – 2 September, 2000, Chicago)	July 2000
951	Vainchtein, D. L., and H. Aref	Morphological transition in compressible foam—*Physics of Fluids* **13**, 2152–2160 (2001)	July 2000
952	Chaïeb, S., E. Sato-Matsuo, and T. Tanaka	Shrinking-induced instabilities in gels	July 2000
953	Riahi, D. N., and A. T. Hsui	A theoretical investigation of high Rayleigh number convection in a nonuniform gravitational field—*International Journal of Pure and Applied Mathematics*, in press (2003)	Aug. 2000

List of Recent TAM Reports (cont'd)

No.	Authors	Title	Date
954	Riahi, D. N.	Effects of centrifugal and Coriolis forces on a hydromagnetic chimney convection in a mushy layer—*Journal of Crystal Growth* **226**, 393–405 (2001)	Aug. 2000
955	Fried, E.	An elementary molecular-statistical basis for the Mooney and Rivlin–Saunders theories of rubber-elasticity—*Journal of the Mechanics and Physics of Solids* **50**, 571–582 (2002)	Sept. 2000
956	Phillips, W. R. C.	On an instability to Langmuir circulations and the role of Prandtl and Richardson numbers—*Journal of Fluid Mechanics* **442**, 335–358 (2001)	Sept. 2000
957	Chaïeb, S., and J. Sutin	Growth of myelin figures made of water soluble surfactant—Proceedings of the 1st Annual International IEEE–EMBS Conference on Microtechnologies in Medicine and Biology (October 2000, Lyon, France), 345–348	Oct. 2000
958	Christensen, K. T., and R. J. Adrian	Statistical evidence of hairpin vortex packets in wall turbulence—*Journal of Fluid Mechanics* **431**, 433–443 (2001)	Oct. 2000
959	Kuznetsov, I. R., and D. S. Stewart	Modeling the thermal expansion boundary layer during the combustion of energetic materials—*Combustion and Flame*, in press (2001)	Oct. 2000
960	Zhang, S., K. J. Hsia, and A. J. Pearlstein	Potential flow model of cavitation-induced interfacial fracture in a confined ductile layer—*Journal of the Mechanics and Physics of Solids*, **50**, 549–569 (2002)	Nov. 2000
961	Sharp, K. V., R. J. Adrian, J. G. Santiago, and J. I. Molho	Liquid flows in microchannels—Chapter 6 of *CRC Handbook of MEMS* (M. Gad-el-Hak, ed.) (2001)	Nov. 2000
962	Harris, J. G.	Rayleigh wave propagation in curved waveguides—*Wave Motion* **36**, 425–441 (2002)	Jan. 2001
963	Dong, F., A. T. Hsui, and D. N. Riahi	A stability analysis and some numerical computations for thermal convection with a variable buoyancy factor—*Journal of Theoretical and Applied Mechanics* **2**, 19–46 (2002)	Jan. 2001
964	Phillips, W. R. C.	Langmuir circulations beneath growing or decaying surface waves—*Journal of Fluid Mechanics* (submitted)	Jan. 2001
965	Bdzil, J. B., D. S. Stewart, and T. L. Jackson	Program burn algorithms based on detonation shock dynamics—*Journal of Computational Physics* (submitted)	Jan. 2001
966	Bagchi, P., and S. Balachandar	Linearly varying ambient flow past a sphere at finite Reynolds number: Part 2—Equation of motion—*Journal of Fluid Mechanics* (submitted)	Feb. 2001
967	Cermelli, P., and E. Fried	The evolution equation for a disclination in a nematic fluid—*Proceedings of the Royal Society A* **458**, 1–20 (2002)	Apr. 2001
968	Riahi, D. N.	Effects of rotation on convection in a porous layer during alloy solidification—Chapter 12 in *Transport Phenomena in Porous Media* (D. B. Ingham and I. Pop, eds.), 316–340 (2002)	Apr. 2001
969	Damljanovic, V., and R. L. Weaver	Elastic waves in cylindrical waveguides of arbitrary cross section—*Journal of Sound and Vibration* (submitted)	May 2001
970	Gioia, G., and A. M. Cuitiño	Two-phase densification of cohesive granular aggregates—*Physical Review Letters* **88**, 204302 (2002) (in extended form and with added co-authors S. Zheng and T. Uribe)	May 2001
971	Subramanian, S. J., and P. Sofronis	Calculation of a constitutive potential for isostatic powder compaction—*International Journal of Mechanical Sciences* (submitted)	June 2001
972	Sofronis, P., and I. M. Robertson	Atomistic scale experimental observations and micromechanical/continuum models for the effect of hydrogen on the mechanical behavior of metals—*Philosophical Magazine* (submitted)	June 2001
973	Pushkin, D. O., and H. Aref	Self-similarity theory of stationary coagulation—*Physics of Fluids* **14**, 694–703 (2002)	July 2001

List of Recent TAM Reports (cont'd)

No.	Authors	Title	Date
974	Lian, L., and N. R. Sottos	Stress effects in ferroelectric thin films—*Journal of the Mechanics and Physics of Solids* (submitted)	Aug. 2001
975	Fried, E., and R. E. Todres	Prediction of disclinations in nematic elastomers—*Proceedings of the National Academy of Sciences* **98**, 14773–14777 (2001)	Aug. 2001
976	Fried, E., and V. A. Korchagin	Striping of nematic elastomers—*International Journal of Solids and Structures* **39**, 3451–3467 (2002)	Aug. 2001
977	Riahi, D. N.	On nonlinear convection in mushy layers: Part I. Oscillatory modes of convection—*Journal of Fluid Mechanics* **467**, 331–359 (2002)	Sept. 2001
978	Sofronis, P., I. M. Robertson, Y. Liang, D. F. Teter, and N. Aravas	Recent advances in the study of hydrogen embrittlement at the University of Illinois—Invited paper, Hydrogen–Corrosion Deformation Interactions (Sept. 16–21, 2001, Jackson Lake Lodge, Wyo.)	Sept. 2001
979	Fried, E., M. E. Gurtin, and K. Hutter	A void-based description of compaction and segregation in flowing granular materials—*Proceedings of the Royal Society of London A* (submitted)	Sept. 2001
980	Adrian, R. J., S. Balachandar, and Z.-C. Liu	Spanwise growth of vortex structure in wall turbulence—*Korean Society of Mechanical Engineers International Journal* **15**, 1741–1749 (2001)	Sept. 2001
981	Adrian, R. J.	Information and the study of turbulence and complex flow—*Japanese Society of Mechanical Engineers Journal B*, in press (2002)	Oct. 2001
982	Adrian, R. J., and Z.-C. Liu	Observation of vortex packets in direct numerical simulation of fully turbulent channel flow—*Journal of Visualization*, in press (2002)	Oct. 2001
983	Fried, E., and R. E. Todres	Disclinated states in nematic elastomers—*Journal of the Mechanics and Physics of Solids* **50**, 2691–2716 (2002)	Oct. 2001
984	Stewart, D. S.	Towards the miniaturization of explosive technology—Proceedings of the 23rd International Conference on Shock Waves (2001)	Oct. 2001
985	Kasimov, A. R., and Stewart, D. S.	Spinning instability of gaseous detonations—*Journal of Fluid Mechanics* (submitted)	Oct. 2001
986	Brown, E. N., N. R. Sottos, and S. R. White	Fracture testing of a self-healing polymer composite—*Experimental Mechanics* (submitted)	Nov. 2001
987	Phillips, W. R. C.	Langmuir circulations—*Surface Waves* (J. C. R. Hunt and S. Sajjadi, eds.), in press (2002)	Nov. 2001
988	Gioia, G., and F. A. Bombardelli	Scaling and similarity in rough channel flows—*Physical Review Letters* **88**, 014501 (2002)	Nov. 2001
989	Riahi, D. N.	On stationary and oscillatory modes of flow instabilities in a rotating porous layer during alloy solidification—*Journal of Porous Media*, in press (2002)	Nov. 2001
990	Okhuysen, B. S., and D. N. Riahi	Effect of Coriolis force on instabilities of liquid and mushy regions during alloy solidification—*Physics of Fluids* (submitted)	Dec. 2001
991	Christensen, K. T., and R. J. Adrian	Measurement of instantaneous Eulerian acceleration fields by particle-image accelerometry: Method and accuracy—*Experimental Fluids* (submitted)	Dec. 2001
992	Liu, M., and K. J. Hsia	Interfacial cracks between piezoelectric and elastic materials under in-plane electric loading—*Journal of the Mechanics and Physics of Solids*, in press (2002)	Dec. 2001
993	Panat, R. P., S. Zhang, and K. J. Hsia	Bond coat surface rumpling in thermal barrier coatings—*Acta Materialia* **51**, 239–249 (2003)	Jan. 2002
994	Aref, H.	A transformation of the point vortex equations—*Physics of Fluids* **14**, 2395–2401 (2002)	Jan. 2002
995	Saif, M. T. A, S. Zhang, A. Haque, and K. J. Hsia	Effect of native Al_2O_3 on the elastic response of nanoscale aluminum films—*Acta Materialia* **50**, 2779–2786 (2002)	Jan. 2002
996	Fried, E., and M. E. Gurtin	A nonequilibrium theory of epitaxial growth that accounts for surface stress and surface diffusion—*Journal of the Mechanics and Physics of Solids*, in press (2002)	Jan. 2002

List of Recent TAM Reports (cont'd)

No.	*Authors*	*Title*	*Date*
997	Aref, H.	The development of chaotic advection—*Physics of Fluids* **14**, 1315–1325 (2002); see also *Virtual Journal of Nanoscale Science and Technology*, 11 March 2002	Jan. 2002
998	Christensen, K. T., and R. J. Adrian	The velocity and acceleration signatures of small-scale vortices in turbulent channel flow—*Journal of Turbulence*, in press (2002)	Jan. 2002
999	Riahi, D. N.	Flow instabilities in a horizontal dendrite layer rotating about an inclined axis—*Proceedings of the Royal Society of London A* (submitted)	Feb. 2002
1000	Kessler, M. R., and S. R. White	Cure kinetics of ring-opening metathesis polymerization of dicyclopentadiene—*Journal of Polymer Science A* **40**, 2373–2383 (2002)	Feb. 2002
1001	Dolbow, J. E., E. Fried, and A. Q. Shen	Point defects in nematic gels: The case for hedgehogs—*Proceedings of the National Academy of Sciences* (submitted)	Feb. 2002
1002	Riahi, D. N.	Nonlinear steady convection in rotating mushy layers—*Journal of Fluid Mechanics*, in press (2003)	Mar. 2002
1003	Carlson, D. E., E. Fried, and S. Sellers	The totality of soft-states in a neo-classical nematic elastomer—*Proceedings of the Royal Society A* (submitted)	Mar. 2002
1004	Fried, E., and R. E. Todres	Normal-stress differences and the detection of disclinations in nematic elastomers—*Journal of Polymer Science B: Polymer Physics* **40**, 2098–2106 (2002)	June 2002
1005	Fried, E., and B. C. Roy	Gravity-induced segregation of cohesionless granular mixtures—*Lecture Notes in Mechanics*, in press (2002)	July 2002
1006	Tomkins, C. D., and R. J. Adrian	Spanwise structure and scale growth in turbulent boundary layers—*Journal of Fluid Mechanics* (submitted)	Aug. 2002
1007	Riahi, D. N.	On nonlinear convection in mushy layers: Part 2. Mixed oscillatory and stationary modes of convection—*Journal of Fluid Mechanics* (submitted)	Sept. 2002
1008	Aref, H., P. K. Newton, M. A. Stremler, T. Tokieda, and D. L. Vainchtein	Vortex crystals—*Advances in Applied Mathematics* **39**, in press (2002)	Oct. 2002
1009	Bagchi, P., and S. Balachandar	Effect of turbulence on the drag and lift of a particle—*Physics of Fluids* (submitted)	Oct. 2002
1010	Zhang, S., R. Panat, and K. J. Hsia	Influence of surface morphology on the adhesive strength of aluminum/epoxy interfaces—*Journal of Adhesion Science and Technology* (submitted)	Oct. 2002
1011	Carlson, D. E., E. Fried, and D. A. Tortorelli	On internal constraints in continuum mechanics—*Journal of Elasticity* (submitted)	Oct. 2002
1012	Boyland, P. L., M. A. Stremler, and H. Aref	Topological fluid mechanics of point vortex motions—*Physica D* **175**, 69–95 (2002)	Oct. 2002
1013	Bhattacharjee, P., and D. N. Riahi	Computational studies of the effect of rotation on convection during protein crystallization—*Journal of Crystal Growth* (submitted)	Feb. 2003
1014	Brown, E. N., M. R. Kessler, N. R. Sottos, and S. R. White	*In situ* poly(urea-formaldehyde) microencapsulation of dicyclopentadiene—*Journal of Microencapsulation* (submitted)	Feb. 2003
1015	Brown, E. N., S. R. White, and N. R. Sottos	Microcapsule induced toughening in a self-healing polymer composite—*Journal of Materials Science* (submitted)	Feb. 2003
1016	Kuznetsov, I. R., and D. S. Stewart	Burning rate of energetic materials with thermal expansion—*Combustion and Flame* (submitted)	Mar. 2003